Polymer Bulletin 61, 759–769 (2008)
DOI 10.1007/s00289-008-1001-z

Polymer Bulletin

Characterization by Dynamic Thermal Methods of Some Bis-Azopolyethers with Flexible Spacer

Gabriela Lisa (✉)[1], N. Hurduc[1], S. Alăzăroaie[1], Natalia Hurduc[2]

[1]„Gh. Asachi" Technical University Iasi, Faculty of Chemical Engineering, B-dul D. Mangeron 71, Iasi-700050, Romania
[2]„Al. I. Cuza" University Iasi, Faculty of Chemistry, B-dul Carol I 11, Iasi-700506, Romania

E-mail: gapreot@yahoo.com, gapreot@ch.tuiasi.ro; Fax: (40) 232-271311

Received: 19 March 2008 / Revised version: 1 September 2008 / Accepted: 2 September 2008
Published online: 20 September 2008 –

Summary

The work presents the characterization by dynamic thermal methods of some bis-azopolyethers with flexible spacer. A MOM-Budapest derivatograph was used for the thermal analysis that enables the simultaneous registration of the thermogravimetric curve (TG), of the derivative thermogravimetric curve (DTG) and of the differential thermal analysis (DTA). The registrations were made in air – static conditions, at different heating rates (5, 10, 15, 20K/min) by keeping constant the other operational parameters in order to obtain comparable data. The study led to some conclusions about the structure - thermostability - degradation mechanism.
The thermostability is determined by the presence of the azo groups, but it may be modified, depending on the nature and the relevance of the co-monomer. The mechanism of the thermal degradation is complex, by successive reactions, the fragmentation of the chain being influenced by the chemical structure and the heating rate.

Keywords

bis-azopolyethers with flexible spacer, thermostability, degradation mechanism, kinetic characteristics

Introduction

Thermal stability is an important factor that affects the use of a new compound in technological applications, particularly in the fields where high-temperature processing is required [1]. In the case of liquid crystals, besides the necessary physical properties, fluidity, optic anisotropy, low viscosity, the compounds should be thermally stable on the temperature range within the liquid crystal state. When the isotropisation temperature exceeds the decomposition temperature, it is necessary to study the thermal stability of these compounds [2-4]. Such behaviour is characteristic

also to bis-azopolyethers with flexible spacer characterized in this paper. The analysis of their thermal behaviour leads finally to the determination of the dependence structure - thermostability - degradation mechanism. Furthermore, the polymers with azo-benzene groups in the main or secondary chain are received a great attention lately due to the potential use in photonics, to obtain nano-structured surfaces, in laser nano-handling, the controlled drug release, energy storage etc. [5-11]. The response of the azo-polymeric materials to light stimuli lays on the photo-izomerization capacity of the azobenzenic groups, able to pass reversibly from a trans-stable energetic configuration to one cis, meta-stable. The configuration changes of the azo groups induce severe changes of the geometry of molecular chains, particularly when the chromophore groups are in the main chain [12]. Because a large part of the applications of the azo-polymeric materials involve their interaction with laser irradiation sources, the determination of the thermal stability limits of polymers becomes a compulsory requirement, even if the material does not have properties of liquid crystal.

In order to achieve a deeper understanding of the thermal behaviour of these aromatic polyethers [13-19], some aromatic bis-azopolyethers with flexible spacer of methylenic type have been analysed. The factors that had been studied were the influence of structure and the heating rates. For this purpose, two groups of co-polyethers synthesized by phase transfer catalysis method were analysed [20, 21]. The monomer with azo groups was kept unchanged while the co-monomer and molar ratios of copolymerization were changed. The thermogravimetric data were processed by differential and integral methods in order to obtain more information on the mechanism of thermal degradation and to assess some kinetic characteristics under various conditions: at low degrees of conversion, at the highest degradation rate, per stages or depending on the conversion degree [22-24].

Experiment

The bis-azopolyethers analyzed by dynamic thermal methods were synthesized by the phase transfer catalysis under the following conditions: temperature: 85°C, catalyst: tetrabutylammonium bromide, the concentration of NaOH 40 %, organic solvent: nitrobenzene, reaction time: 5 hours. The reaction scheme is presented as follows:

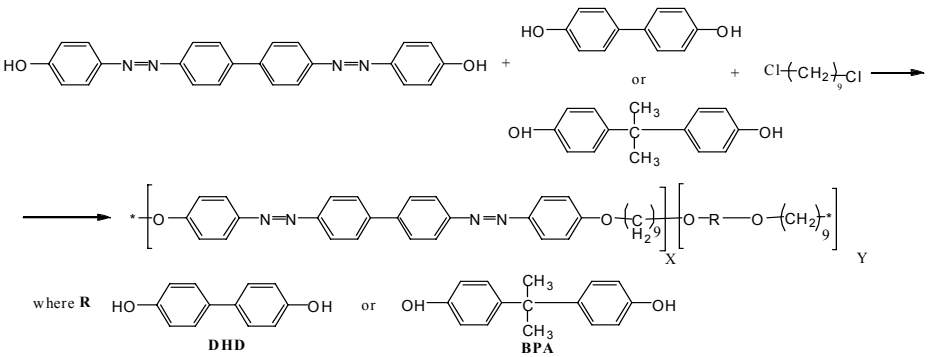

The analyzed samples are presented in Table 1.

Table 1. The analyzed samples by dynamic thermal methods

Sample	X/Y	Structural unit	Group
1	3/1	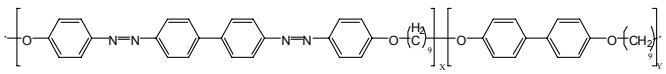	**A**
2	1/1		
3	1/3		
4	3/1	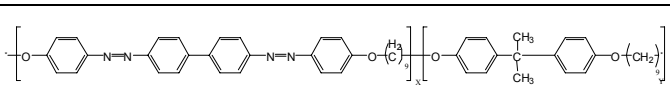	**B**
5	1/1		
6	1/3		

A MOM-Budapest Paulik-Erdey derivatograph that enables the simultaneous registration of the temperature (T) thermogravimetric analysis (TG), derivative thermogravimetric analysis (DTG) and differential thermal analysis (DTA) was used. The recordings were made in the air – static conditions, at different heating rates (5, 10, 15, 20ºC /min), temperature domain of 20-1000ºC/min, sample weight of 50mg, and by using powdered samples in platinum crucibles and as reference material α-Al_2O_3.

Results and discussions

According to the thermograms from fig. 1 and 2, the thermal degradation take place in three stages, being accompanied by endo- and exothermal effects, irrespective of the chemical structure or heating rate.

The thermogravimetric characteristics in the table 1 show close temperature ranges for the three degradation stages, while the mass losses depend on the structure and less on the heating rate.

The thermal characteristics of table 2 show the enhancement of the thermal stability for the samples of the group B, favoured by the nature of the co-monomer and its relevance.

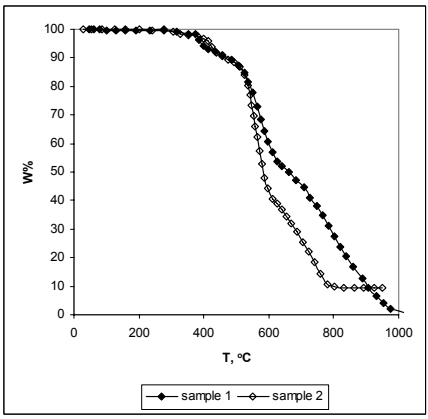

a) TG curves

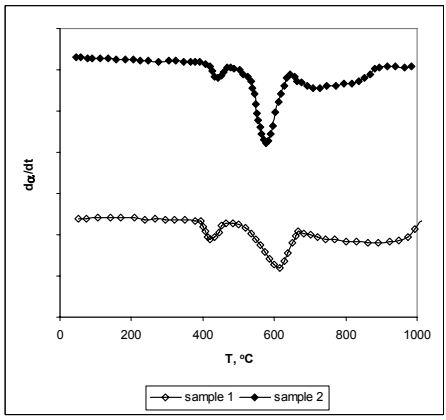

b) DTG curves

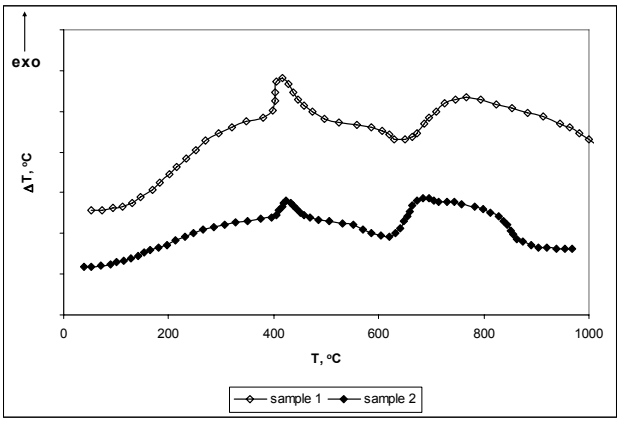

c) DTA curves

Figure 1. The thermograms of group **A** samples at heating rate 10ºC /min

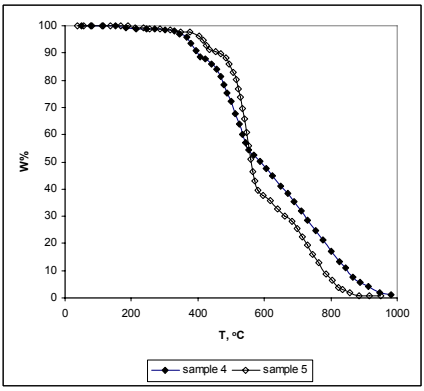

a) TG curves

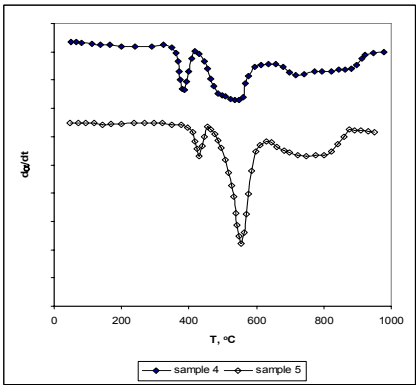

b) DTG curves

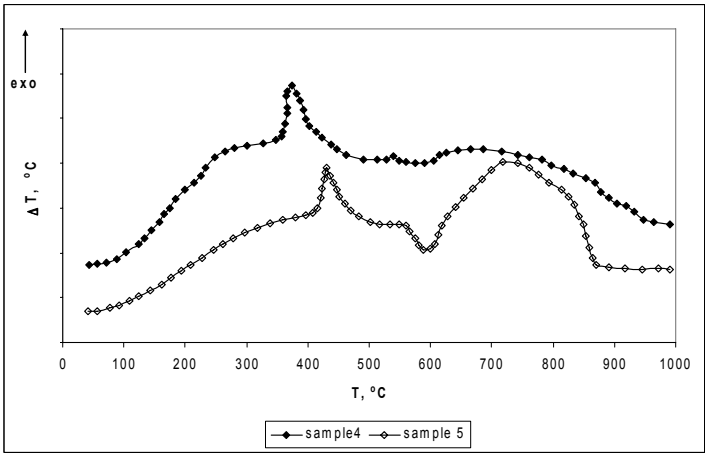

c) DTA curves

Figure 2. The thermograms of group **B** samples at heating rate 10ºC /min

Table 1. Thermogravimetric characteristics at various heating rates

Sample	dT/dt (K/min)	ΔT_1 (ºC)	W_1 (%)	ΔT_2 (ºC)	W_2 (%)	ΔT_3 (ºC)	W_3 (%)
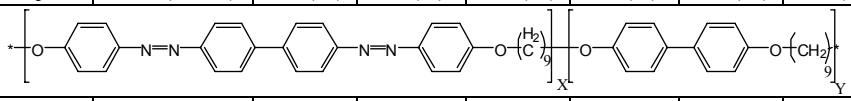							
1	10	300-410	10.90	410-580	33.18	580-850	50.90
	15	290-390	9.32	390-600	38.98	600-900	51.35
	20	300-380	8.33	380-620	44.69	620-880	46.91
2	10	310-400	7.14	400-590	54.28	590-860	38.57
	15	310-430	7.00	430-605	58.00	605-810	35.00
	20	320-420	7.67	420-620	59.61	620-870	32.69
3	10	300-400	9.67	400-600	61.29	600-800	29.00
	15	310-400	9.80	400-600	60.65	600-800	29.54
	20	320-420	6.25	420-600	66.66	600-800	27.00
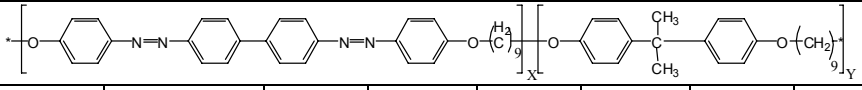							
4	10	320-400	8.69	400-560	38.00	560-800	53.00
	15	320-400	11.29	400-610	43.54	610-830	45.16
	20	320-400	9.16	400-610	45.83	610-820	45.00
5	5	300-420	9.25	420-570	54.16	570-800	36.06
	10	340-420	10.14	420-660	56.50	660-870	33.00
	15	350-420	8.20	410-580	52.00	580-880	39.80
	20	340-410	9.82	410-590	59.92	510-840	30.25
6	10	320-430	7.54	430-600	70.38	600-820	21.51
	15	380-460	5.66	460-610	69.81	610-820	24.52
	20	360-440	8.97	440-590	67.94	590-810	23.19

ΔT – temperature range; W – the weight loss corresponding to the degradation stage

Table 2. Thermal characteristics depending on the structure and the heating rate at various degrees of transformation

Sample	dT/dt (K/min)	T_i (ºC)	$T_{10\%}$ (ºC)	$T_{20\%}$ (ºC)	$T_{50\%}$ (ºC)	$T_{80\%}$ (ºC)	T_{M1} (ºC)	T_{M2} (ºC)
1	10	300	397	542	652	792	340	520
	15	290	417	487	607	792	345	530
	20	300	387	472	562	792	350	535
2	10	310	366	507	537	712	370	525
	15	310	366	507	537	712	380	530
	20	320	366	507	537	712	390	535
3	10	300	412	432	507	642	380	515
	15	310	487	507	537	682	385	530
	20	320	467	492	557	617	390	535
4	10	320	377	447	567	687	350	520
	15	320	377	497	597	767	355	530
	20	320	377	447	597	767	360	550
5	10	340	427	502	521	717	380	510
	15	350	427	502	547	820	390	515
	20	340	427	502	527	694	395	525
6	10	320	447	487	487	627	410	515
	15	380	447	532	562	647	415	520
	20	360	447	517	532	627	425	630

T_i – initial degradation temperature; T_α – corresponding temperature at various weight loss: α = 10, 20, 50, 80%; T_M – temperature at maximum degradation rate

The corresponding temperatures at various degrees of transformation obey no laws, which suggest that the chain is fragmented depending on its chemical structure and heating rate. Furthermore, the temperature corresponding to the highest degradation rate is influenced by structure and operation conditions. These findings show the complexity of the degradation process.
In order to obtain information on the mechanism of thermal degradation, the weight fraction loss calculations has been made for the fragmentation of the chain that were compared to the ATG data as it results from table 3. Taking into consideration the sequences of structures from Table 3 and assuming that the fragmentation takes place in the order: azo groups, spacer and aromatic rings a good agreement between the experimental percentual loss after each stage and the theoretic assumption was obtained.
Taking into account the assumption regarding the degradation process discussed earlier a general scheme of thermal degradation of group A and B polymers was imagined.

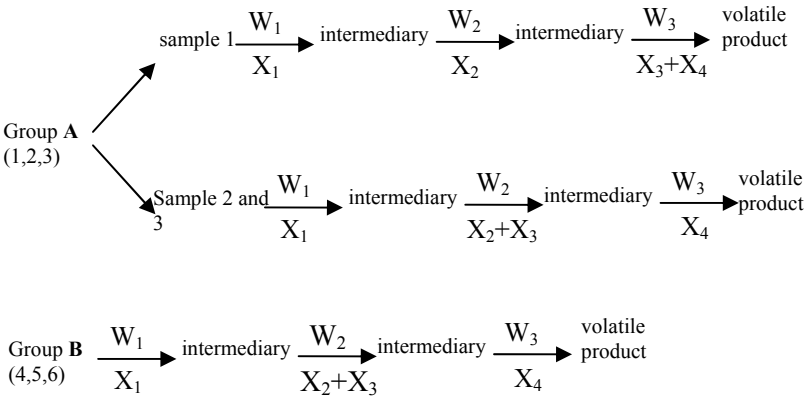

In order to obtain some additional data regarding the thermal degradation mechanism, the kinetic processing of the thermogravimetric data by the methods based on the model of the reaction order was performed. The application of the Kissinger method [23] that enables the calculation of the activation energy under conditions of highest degradation rate, gives rise to the values provided in table 4.
Generally, for the first degradation stage, higher values than for the second degradation stage are obtained. The differences are small, except for the sample 2. Analyzing the temperature range in which the temperature corresponding to the highest rate and the activation energy are comprised, a dependency was observed. The increase of ΔT corresponds to lower activation rates.
To assess the activation energy on the entire degradation range, we applied the Coats-Redfern method [24], obtaining the values in table 5.
The kinetic characteristics confirm the complexity of the degradation mechanism. The activation energies are lower in the first and the last degradation stage, in agreement with the scheme proposed under the ATG data. In the first stage, nitrogen is lost, coming from the azo groups that are the most unstable to the thermal attack, requiring a low energetic consumption, compared to the second stage in which the spacer is fragmented and some aromatic cycles with a higher energetic consumption occur, in

Table 3. Mass losses calculated in comparison with the ATG data

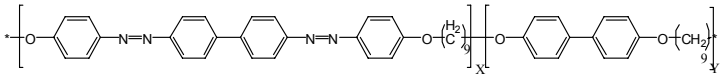

Sample		X/Y	dT/dt K/min	ATG data			Calculation data				Observation	
				W_1%	W_2%	W_3%	X_1 %	X_2 %	X_3 %	X_4 %		
A	1	3/1	10	10.90	33.18	50.90	9.00	33.90	8.15	43.92	$W_1 \cong X_1$ $W_2 \cong X_2$ $W_3 \cong X_3+X_4$	X_1=azoth X_2=spacer X_3= 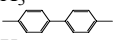 X_4= remainder aromatic cycles
			15	9.32	38.98	51.35						
			20	8.33	44.64	46.96						
	2	1/1	10	7.14	54.28	29.00	6.76	38.16	18.36	36.72	$W_1 \approx X_1$ $W_2 \approx X_2+X_3$ $W_3 \approx X_4$	
			15	7.00	58.00	29.51						
			20	7.69	51.61	27.00						
	3	1/3	10	7.67	61.29	29.00	3.87	49.64	31.49	20.99	$W_1 > X_1$ $W_2 > X_2+$ $X_3 W_3 > X_4$	
			15	9.80	60.65	29.51						
			20	6.25	66.66	27.00						

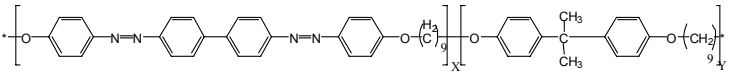

B	4	3/1	10	8.69	38.00	53.00	9.65	33.14	8.50	47.82	$W_1 \approx X_1$ $W_2 \approx X_2+X_3$ $W_3 \approx X_4$	X_1=N_2+2CH_3 X_2=spacer+O_2 X_3= 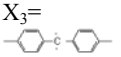 X_4= remainder aromatic cycles
			15	11.29	42.54	45.16						
			20	9.16	45.83	45.00						
	5	1/1	5	9.25	54.16	36.06	9.14	36.28	18.83	34.90	$W_1 \approx X_1$ $W_2 \leq X_2+X_3$ $W_3 < X_4$	
			10	10.14	56.10	33.00						
			15	8.20	52.00	39.80						
			20	9.82	59.82	30.35						
	6	1/3	10	7.59	70.38	21.51	8.49	40.10	31.20	19.28	$W_1 \approx X_1$ $W_2 \approx X_2+X_3$ $W_3 > X_4$	
			15	5.66	69.81	24.52						
			20	8.97	67.84	23.19						

Table 4. Activation energy assessed by the Kissinger method

Sample	X/Y	E, kJ/mol		Group	ΔT_1	ΔT_2
		Stage 1	Stage 2			
1	3/1	196	171	**A**	10	15
2	1/1	139	268		20	10
3	1/3	280	101		10	20
4	3/1	157	107	**B**	10	30
5	1/1	164	156		15	15
6	1/3	184	172		15	15

Comonomer group A: DHD; Comonomer group B: BPA

compliance with the values of the apparent activation energies. The last stage corresponds to a thermal oxidation process accompanied by a strong exothermal process, requiring a lower energetic consumption compared with the second stage. In the last stage, the apparent activation energies are closer, showing a similar process.

Table 5. Kinetic characteristics assessed via the Coats-Redfern method

Sample	X/Y	dT/dt (K/min)	Stage I		Stage II		Stage III	
			n	E (KJ/mol)	n	E (KJ/mol)	n	E (KJ/mol)
1	3/1	10	0	99	1	130	0	87
		15	0	103	1	100	0	79
		20	0	91	1	124	0	90
2	1/1	10	0	97	1	99	0	84
		15	0	100	1	175	0	80
		20	0	104	1	158	0	61
3	1/3	10	0	54	1	180	0	86
		15	0	85	1	233	0	80
		20	0	70	1	191	0	90
4	3/1	10	0	74	1	120	0	60
		15	0	45	1	112	0	87
		20	0	64	1	99	0	86
5	1/1	10	0	102	1	127	0	84
		15	0	69	1	223	0	64
		20	0	107	1	197	0	90
6	1/3	10	0	86	1	174	0	74
		15	0	66	1	184	0	102
		20	0	49	1	308	0	114

n – reaction order, E– apparent activation energy

Table 6. Kinetic parameters assessed by the Freeman-Caroll method for various heating rates (for the temperature range ΔT_2)

Sample	X/Y	dT/dt (K/min)	n	E (kJ/mol)	lnA	Sp	T_{cr}(K)	T_M(K)
1	3/1	10	1	147	26.58	6.59	840	793
		15	1	287	43.15	6.68	810	803
		20	1	112	17.24	6.67	869	808
2	1/1	10	1	149	24.46	6.80	845	798
		15	1	170	27.18	6.25	830	803
		20	1	160	23.81	6.71	827	808
3	1/3	10	1	293	45.17	6.48	800	788
		15	1	335	50.21	6.80	805	803
		20	1	405	61.04	6.55	803	808
4	3/1	10	1	255	38.22	6.57	808	793
		15	3	217	32.78	6.63	826	813
		20	2.5	205	30.70	6.67	838	823
5	1/1	5	2	272	42.32	6.42	-	773
		10	1	229	34.95	6.56	812	793
		15	2	242	36.07	6.70	788	788
		20	1	217	32.66	6.44	808	803
6	1/3	10	1	372	57.73	6.44	787	783
		15	1	313	46.61	6.71	795	793
		20	2	303	45.00	6.73	798	803

n – reaction order, E– apparent activation energy, A- preexponential factor, Sp = E/lnA – compensation parameter, T_{cr} – critical temperature, T_M – temperature corresponding to the highest degradation rate

There is a good agreement between the kinetic parameters and the proposed degradation mechanism.
The careful analysis of the kinetic characteristics showed an important part played by the spacer during thermal degradation. Starting from this finding, we applied the Freeman – Carroll method [22] that considers the interval up to the reaching of the highest degradation rate. The calculated kinetic parameters are presented in table 6 that includes the compensation parameter and the critical temperature calculated with the Gorbachev equation [26].
The activation energy and the reaction order are influenced by the molar relation of copolymerization and the heating rate, highlighting the influence of the spacer in small molecular compounds with a variable number of carbon atoms. The compensation parameter within the limit of the experimental errors shows the same type of degradation mechanism. The critical temperature is close to the temperature corresponding to the highest degradation rate.
The application of the Flynn-Wall method [25] of interpretation of the thermogravimetric data enables the determination of the dependence between the activation energy and the conversion degree. For the analyzed samples, the Flynn-Wall charts are observed to be "atypical". Examples of charts for samples in group A are shown in the figures 3-5.
Deviations instead of parallel lines with a negative slope at various conversion degrees were observed; additionally points of inflexion that show the change of the reaction mechanism with the heating rate for the samples 1 and 3 were obtained. In the chart $\alpha = f(T)$ the interposition of the curve corresponding to the heating rate of 20K/min from 10 to 15K/min was noticed.

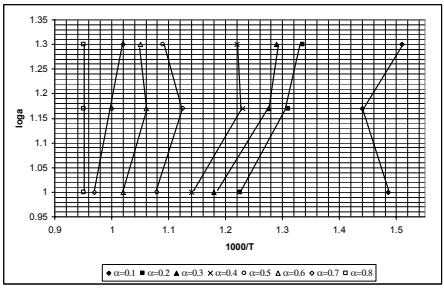

Figure 3. Flynn-Wall chart for the sample 1

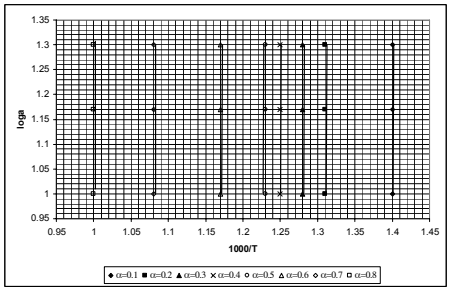

Figure 4. Flynn-Wall chart for the sample 2

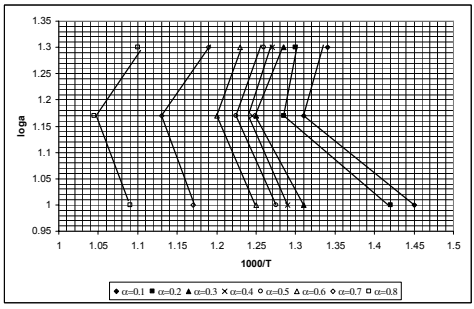

Figure 5. Flynn-Wall chart for the sample 3

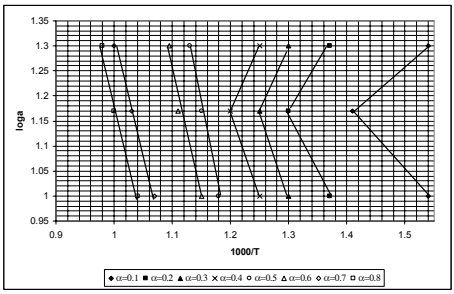

Figure 6. Flynn-Wall chart for the sample 4

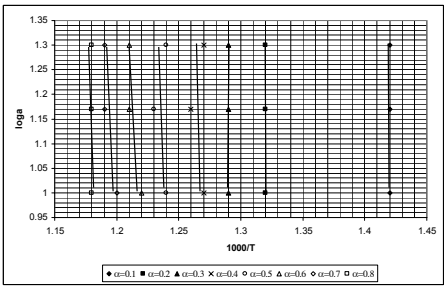

Figure 7. Flynn-Wall chart for the sample 5

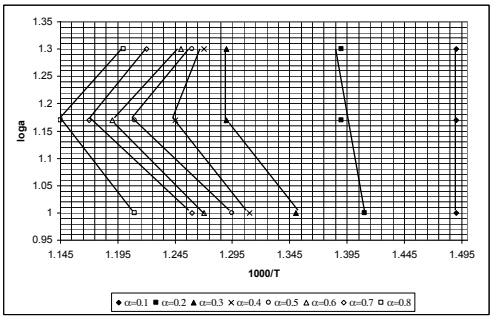

Figure 8. Flynn-Wall chart for the sample 6

For the sample 2 parallel lines occur and there are no essential changes with the heating rate. The curves $\alpha = f(T)$ are overlapping for the aforesaid heating rates.
For the samples of the group B according to the fig. 6-8, a similar behaviour with the samples 1 and 3 was observed.
By correlating the kinetic characteristics with the thermogravimetric ones, we can see the complexity of the degradation mechanism in which an important part is played by the spacer that contains a large number of methylenic groupings, in which case the behaviour may be compared with polyethylene [27].

Conclusions

The conducted study leads to some conclusions regarding the structure - thermostability - degradation mechanism.
The thermostability is determined by the presence of the azo groups, but it may change, depending on the nature of the co-monomer: the polyether of the groups B having a higher thermostability than those of the groups A. The nature and the percent of the co-monomer influence the thermostability, while the heating rate plays an insignificant part.
The mechanism of thermal degradation is complex, by successive reactions, the fragmentation of the chain being influenced by the chemical structure and by the heating rate.
The azo-polymers present a good thermal stability, the processes of degradation being triggered at temperatures higher than 300°C. This recommends their use in obtaining

nano-structured surfaces, ordered surfaces, laser nano-handling, (temperatures of the film surface do not exceed 100°C).

Acknowledgement. The authors would like to thank to the Ministry of Education for the financial support (Contract CNCSIS 100 GR/2007, Cod CNCSIS 277). The thermal stability studies were effectuated on the Interdisciplinary Research Platform for Multifunctional, High Performance Polymers (Contract no. 69/2006 CNCSIS).

References

1. Hamciuc C, Vlad-Bubulac T, Petreus O, Lisa G (2008) Polym Bull 60: 1436
2. Martinez J C A, Novack K M, Gomes A S (1996) Polym Bull 37: 497
3. Kobmel G, Lundt B (1994) Polym Bull 33: 497
4. Kobmel G, Lundt B (1995) Polym Bull 33: 503
5. Rochon P, Batalla E, Natansohn A (1995) Appl Phys Lett 66: 136
6. Kim D Y, Tripathy S K, Li L, Kumar J (1995) Appl Phys Lett 66: 1166
7. Yager K, Barett C J (2001) Curr Opin Solid St M 5: 487
8. Karageorgiev P, Neher D, Schultz B, Stiller B, Pietsch U, Giersieg M, Brehmer L (2005) Nat Mater 4: 699
9. Hurduc N, Enea R, Scutaru D, Sacarescu L, Donose B C, Nguyen A V (2007) J Polym Sci A: Polym Chem 45: 4240
10. Zhao Y (2007) Chem Rec 7: 286
11. Folgering J, Kuiper J, de Vies A, Engberts J, Poolman B (2004) Langmuir 20: 6985
12. Strat M, Delibas M, Strat G, Hurduc N, Gurlui S (1998) J Macromol Sci: Part B: Polym Physics –B 37: 387
13. Hurduc N, Damian C, Ţăruş A, Toader V (2005) Cent Eur J Chem 31: 53
14. Damian C, Hurduc N, Lisa G, Alazăroaie S, Hurduc N (2005) Mater Plast 42: 301
15. Damian C, Hurduc N, Hurduc N, Shanks R, Yarovskz I, Pavel D (2003) Comp Mate Sci 27: 393
16. Hurduc N, Creangă A, Pokol G, Norvak C, Scutaru D, Alăzăroaie S, Hurduc N (2002) J Therm Anal Cal 70: 877
17. Hurduc N, Prăjinaru M, Donose B, Pavel D, Hurduc N (2001) Polym Degrad Stab 72: 441
18. Hurduc N, Prăjinaru M, Creangă A, Hurduc N, Alăzăroaie S (2002) Mater Plast 39: 231
19. Prăjinaru M, Hurduc N, Alăzăroaie S, Cătănescu O, Hurduc N (2003) Cent Eur J Chem, 4: 387
20. Alazaroaie S, Catanescu C O, Pavel D, Scutaru D, Toader V, Simionescu C I, Hurduc N (2005) High Perform Polym 17: 149
21. Alazaroaie S, Hurduc N, Scutaru D, Dumitrascu A, Petraru L, Simionescu Cr (2003) J Macromol Sci- Pure Apll Chem 11: 1241
22. Freeman E S, Carroll B (1958) J Phys Chem 62: 314
23. Kissinger H E (1957) Anal. Chem. 29: 1702
24. Coats A W, Redfern J P (1964) Nature 201: 68
25. Flynn J H, Wall L A (1966) Polymer Letter 4: 323
26. Gorbachev V M, Nicolaev A V, Lognienko A (1974) J Thermal Anal 6: 473
27. Schneider I A, Hurduc N, Makromol Chem (1977) 178: 547